Journal of Physics: Conference Series **168** (2009) 012019 doi:10.1088/1742-6596/168/1/012019

Hadron structure and hadronic matter

Elena Santopinto
Istituto Nazionale di Fisica Nucleare, Sezione di Genova
Genova, I-16146 Italy
E-mail: santopinto@ge.infn.it

Abstract. Some of the most relevant and recent results of the italian theoretical groups active in hadronic physics are briefly reviewed.

1. Introduction

The studies of hadron properties can be considered to follow roughly two main approaches. The first one, which can be called microscopic or systematic, starts from the internal hadron dynamics, that is from the quark degrees of freedom and their interactions. The widely accepted framework is of course provided by Quantum ChromoDynamics (QCD), which however can be presently treated only in the perturbative regime (pQCD). A big effort is devoted to the analysis of hadron structure in the Lattice QCD (LQCD): there are now many important results [1] and more are expected in the future, when the computer capabilities will allow to reach the required precision of the calculations in order to extract the hadron properties in a systematic way. This will presumably take still some time and in the meanwhile one can rely on models, eventually based on QCD or LQCD. Moreover chiral perturbation theory can be considered as the low-energy effective field theory of QCD [2]. The second approach, which can be denoted as "phenomenological", uses some parametrization of single hadron properties within a theoretical framework, based on general aspects of quarks and gluons dynamics. The two approaches are not sharply separated, but on the contrary they can be strongly correlated and they are introduced mainly for simplifying the discussion.

Many models have been built and applied to the description of hadron properties. An important class is provided by Constituent Quark Models (CQM), in which quarks are considered as effective internal degrees of freedom and can acquire a mass and even, in certain approaches, a finite size. The idea of quarks as constituent particles of hadrons has been introduced very soon [3]; quark confinement was not yet known and quarks were considered to have a very large mass, thereby supporting a non relativistic approach. The modern version of the non relativistic CQM has been formulated by Isgur and Karl [4] (IK), using a h.o. confinement potential and a hyperfine interaction, which is spin dependent and inspired by the One-Gluon-Exchange mechanism (OGE). The IK model has been subsequently reformulated using a relativistic kinetic energy operator and a three-body linear confinement, inspired by a flux tube approach [5] (CI). Further models have been recently proposed. In the $U(7)$-algebraic model [6], $U(7) \otimes SU_{sf}(6) \otimes SU_c(3)$ is used as spectrum generating algebra for the baryons, that is for the excitation spectrum and other properties, such as elastic form factors and helicity amplitudes. The hypercentral CQM (hCQM) is characterized by a linear confinement and a coulomb-like term [7]; the hypercentral interaction depends on the coordinates of the three quarks and can

include three-body effects. The main feature of the chiral CQM [8] is the quark interaction derived from the exchange of Golstone Bosons (GBE), like pions and kaons. In a recent CQM [9], instanton interactions are introduced in order to describe the baryon properties.
Constituent models have been considerably refined to include consistently relativity, formulating or reformulating them in Instant, Front (called also light cone) or Point Form Dynamics. Bethe-Salpeter approches have been also developed. Now the current main effort is towards a systematic and consistent inclusion of the higher Fock components in order to arrive at a new generation of CQMs.

Besides CQMs, there are various models formulated in a consistent way within chiral theory. Many papers have been written along this line of thought and the interested reader is referred to the abundant literature (see e.g. Ref. [10]). A completely different approach is provided by the instanton liquid model (for a review see [11]).

In the following, the recent work done by the italian theoretical groups in the field of hadron physics will be briefly reviewed, considering that they have used all the tools at disposal at the moment, ranging from LQCD up to phenomenological models.

2. CQMs

The nucleon has a rich spectrum, which however becomes very hard to be studied experimentally in the higher energy part because of the large widths of the states and the increasing overlapping of the various resonances. In any case, the description of the spectrum is the first task of a model builder: it serves to determine a quark interaction to be used for the calculation of other physical quantitites. The form factors (elastic and inelastic) are particularly suited for a test of the models, since they use explicitly the baryon wave functions determined by the description of the spectrum. All the various forms of CQMs are able to reproduce more or less the spectrum, even though they differ in the used potential, in particular in the form of the $SU(6)$ spin flavour breaking interaction. Regarding the elastic form factors the use of a relativistic model is essential [12, 13, 14, 15, 16, 17], while for the helicity amplitudes it seems to be less important[18, 19, 20].

A very important test of the models is provided by the helicity amplitudes for the electromagnetic excitation of the nucleon resonances. The transverse amplitudes, $A_{1/2}$ and $A_{3/2}$, are defined as the matrix elements of the transverse electromagnetic interaction, $H^t_{e.m.}$, between the nucleon, N, and the resonance, B, states:

$$\begin{aligned} A_{1/2} &= \langle B, J', J'_z = \tfrac{1}{2} \, |H_{em}| N, J \; = \; \tfrac{1}{2}, J_z = -\tfrac{1}{2} \, \rangle \\ A_{3/2} &= \langle B, J', J'_z = \tfrac{3}{2} \, |H_{em}| N, J \; = \; \tfrac{1}{2}, J_z = \tfrac{1}{2} \, \rangle \end{aligned} \tag{1}$$

The building of a CQM implies the knowledge of model wave functions and therefore the above matrix elements can be calculated. The results of the IK model were soon available [21], however they were obtained adjusting the proton size to a value of about $0.5fm$ [22]. More recently, results from the CI in the light front approach have been obtained by the Rome group [14]. A systematic study of the helicity amplitudes for the negative parity resonances has been performed within the hCQM [20]; this study is now extended to all resonances with an observable electromagnetic transition strength and to the longitudinal excitation amplitudes as well [23]. In the case of the negative parity non strange resonances, the experimental behaviour is fairly well reproduced by the parameter-free calculations made with the hCQM [20], specially for the S_{11}, whose trend has been predicted in advance with respect to the recent Jlab data [24]. In the medium Q^2 region the theoretical amplitudes are not damped, at variance with the h.o. calculations. This softer dependence is due, in the hCQM calculation, to the presence of the Coulomb-like term in the interaction. At low Q^2, in particular for the $A_{3/2}$ amplitudes, there is a lack of strength, which is however typical of all CQMs [18]. Such discrepancy can be attributed

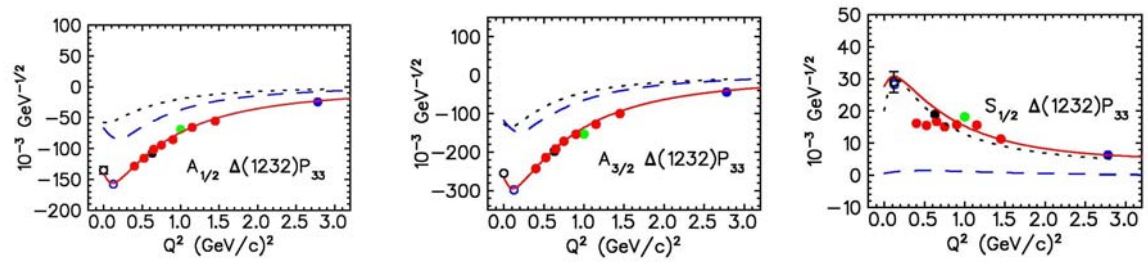

Figure 1. The Q^2 dependence of the $N \to \Delta$ helicity amplitudes. The solid and dashed curves are the results of the superglobal fit with MAID and the predictions of the hCQM, respectively. The dotted lines show the pion cloud contributions calculated with DMT [27]. The data points at finite Q^2 are the results of the Mainz single-Q^2 fits [26]. At $Q^2 = 0$ for $A_{1/2}$ and $A_{3/2}$ the photon couplings from PDG are shown [28].

to the fact that all CQMs miss some fundamental mechanism, such as the quark-antiquark pair production [18]. A confirmation of this statement is provided by a recent analysis performed by a collaboration of the Genoa and Mainz groups [25]. In figure 1 [25] the transition amplitudes for the Δ excitation, calculated with the hCQM, are reported in comparison with a global fit performed by the Mainz group [26]. The meson cloud contributions, evaluated by means of a dynamical model [27], are also reported. Their importance decreases with increasing Q^2, going rapidly to zero, as expected; however, for low Q^2, they are able to fill most of the gap between data and the hCQM results. This feature is quite general, since it happens systematically also for the excitation of higher resonances, such as $P_{11}(1440), S_{11}(1535), D_{13}(1520), F_{15}(1680)$ [25].

To conclude, it should be noted that the proton radius calculated in the hCQM is about $0.5fm$, just the value previously fitted [21, 22] to the $D13$ transition strength. In the outer region, that is for low Q^2, there is a lack of strength, which can be at least partially accounted for by pion cloud contributions. The emerging picture is therefore that of a quark core with a dimension of about $0.5fm$ plus a meson (or sea-quark) cloud.

3. Spin Structure of the Hadrons and Transversity effects

During the last years the interest in spin physics has considerably grown. The study of the nucleon spin structure has made important progress and new ideas and models have been developed. All that can help to learn about the spin structure of hadrons and to describe some spin effects in inclusive and semi-inclusive hadron production, even if still many aspects have to be understood. In parallel with the theoretical efforts, a strong experimental program has already started at RHIC (BRAHMS, PHENIX, STAR), HERA (HERMES), CERN (COMPASS) and KEK (Belle), or is being planned at JLab, JPARC.

The role of intrinsic transverse momentum has received a lot of attention in the context of polarization effects, in particular in transverse Single Spin Asymmetries (SSA) at moderate p_T values. These, contrary to former expectations of pQCD, show sizeable experimental values. It was originally suggested by Sivers [29] (1990) to start from pQCD including transverse momentum effects in parton distribution functions. Subsequently this idea has been developed and extended in a certain number of papers [30, 31, 32, 33, 34, 35].

In particular, a great effort has been devoted, in several steps, to a generalization of the usual collinear pQCD approach with the inclusion of spin and transverse momentum effects by the Torino-Cagliari group [36]. The main steps in the construction, under the assumption of a generalized QCD factorization scheme, and in the refinement of the so-called Generalized Parton Model (GPM), are:

1) The inclusion of spin and transverse momentum dependences in the parton distribution functions (1995) [30, 31];
2) The improved treatment of kinematics with inclusion of transverse momentum effects in the study of unpolarized cross sections and the Sivers effect in pp collisions (2004) [37];
3) The inclusion of all transverse momentum dependences of partons in hadrons and of hadrons produced by fragmenting partons and in the elementary hard interactions computed at leading order with noncollinear kinematics, thus arriving to the GPM [36].

The GPM is based on a factorization scheme, separating the soft, long distance from the hard, short distance contributions. The hard part is computable in perturbative QCD, while information on the soft one has to be extracted from the experiments or modeled. This can be considered a very reasonable starting point (although for non collinear processes factorization has been proved only in particular kinematical situations). Moreover in this scheme leading twist Transverse Momentum Dependent (TMD) distributions keep their partonic interpretation, and are expected to be universal and process-independent. All these reasonable assumptions have, however, to undergo phenomenological scrutiny, considering that this is the best one can do at the moment.

In the context of the GPM the Torino-Cagliari group has started a systematic program of analysis of the existing data, aiming at reproducing all the available data on Single Spin Asymmetries from Semi Inclusive Deep Inelastic Scattering (SIDIS), hadronic collisions and e^+e^- annihilations with a single set of universal TMD distributions. This recently led to the extraction of TMDs, with the possibility of giving very useful predictions for many forthcoming experiments. In particular they were able to obtain, for the first time, the following important results:
i) The simultaneous extraction of the transversity distribution and the Collins fragmentation function [38]. In figure 2 we report the first phenomenological extraction of the transversity distribution for the valence up and down quarks;
ii) Taking into account new higher statistics data from HERMES, COMPASS and Belle, a new phenomenological extraction of the transversity distribution for up and down quarks with a smaller error-band (see figure 3) [39], and of the Collins (see figure 4) [39] and Sivers functions (see figure 5) [40].

By using the Sivers function [41], the transversity distribution and the Collins fragmentation function [38] extracted by means of high quality global fits, within the same scheme, they predict [42] the $p^\uparrow p \to h + X$ single spin asymmetries in remarkable agreement with RHIC experimental data.

Single-spin asymmetries in processes with transversely polarized targets have been measured in proton-proton collisions, $p^\uparrow p \to h + X$ [43], and in semi-inclusive deep inelastic scattering (SIDIS), $l\ p^\uparrow \to l'\ \pi + X$ [44]. Different theoretical approaches [45, 36] have been adopted to study and interpret these asymmetries and make predictions for new possible experiments. In a recent Letter [46], different clear-cut predictions are made for a simple process accessible at RHIC, using the color-gauge QCD invariant formalism [47] and the GPM approach. A weighted asymmetry in the azimuthal distribution of photon-jet pairs, produced in the process $p^\uparrow p \to \gamma$ jet $+X$ with a transversely polarized proton, is studied from both the phenomenological and theoretical point of view. In Ref. [46] different predictions for the asymmetry are obtained. In particular the results with the GPM [36] are compared with the gluonic-pole cross sections calculable in perturbative QCD [47]. The two predictions have opposite signs. Experimental measurements of the asymmetry will therefore test the present understanding of single spin asymmetries.

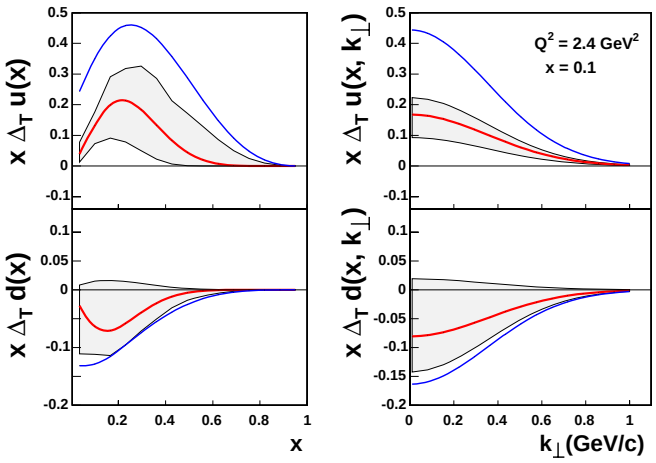

Figure 2. The first phenomenological extraction of the transversity distribution for the up and down quarks from Ref. [38] [APS copyright].

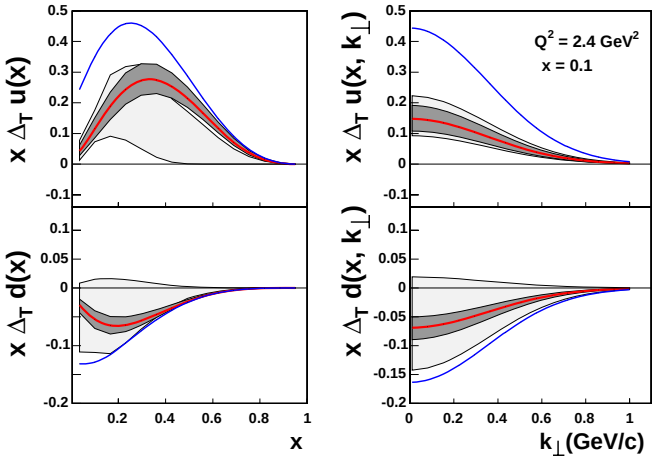

Figure 3. Transversity distribution for the up and down quarks - II extraction [39].

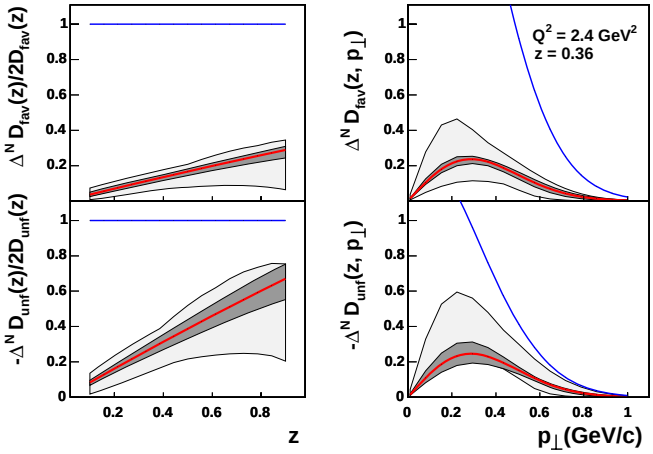

Figure 4. Phenomenological extraction of the Collins function (SIDIS) [39].

3.1. Transverse Momentum Dependent distributions and effective models

As discussed in the previous section, the study of SSA experimental data has required the introduction of a new class of Tranverse Momentum Dependent parton distributions and Fragmentation Functions (FFs). Phenomenologically the most relevant ones are at leading twist, the Sivers and the Boers Mulders distribution functions and the Collins fragmentations functions, since in a factorized pQCD approach they are responsible for most of the azymuthal spin asymmetries in SIDIS, Drell-Yan (DY) processes and e^+e^- annihilations. Factorization theorems have been proved for SIDIS and DY processes in the kinematical regime in which two well distinct energy scales are present: the large scale of the photon virtuality or the invariant mass of the leptonic pair and the low-moderate scale of the transverse momentum p_T of the observed hadron or the leptonic pair in respect to the colliding beams.

Although many models calculations of integrated PFDs are available, there are not so many for TMDs- also called unintegrated PDFs. The Transverse Momentum Dependent Distributions describe the probability of finding in a hadron a parton with longitudinal momentum fraction x and transverse mometum p_T. At leading twist there are eight TMDs [48], three of them surviving when integrated over the transverse momentum and giving rise to parton density, helicity and transversity distributions. Since TMDs are typical non perturbative quantities, they are not directly calculable in QCD, and their modelling requires assumptions on the nucleon wave function.

In Ref.[49] all the leading twist T-even functions were calculated in a light cone spectator model with scalar and axial-vector diquarks. Recently the Pavia group has performed a calculation using light cone three quark wave function [50]. The formalism and the analytic expressions in the SU(6) symmetry limit are derived for the T-even TMDs, studied in a light-cone description of the nucleon with the Fock expansion truncated to three valence quarks [50]. Numerical results for the T-even TMDs are shown in their paper [50] by using the Schlumpf [51] parametrization of the momentum wave function. It is interesting to observe figure 4 of Ref. [50] (see figure 6 of this article) where the Pavia results obtained with both the Schlumpf [51] and the hypercentral wave function [52, 7] are compared with results obtained with other

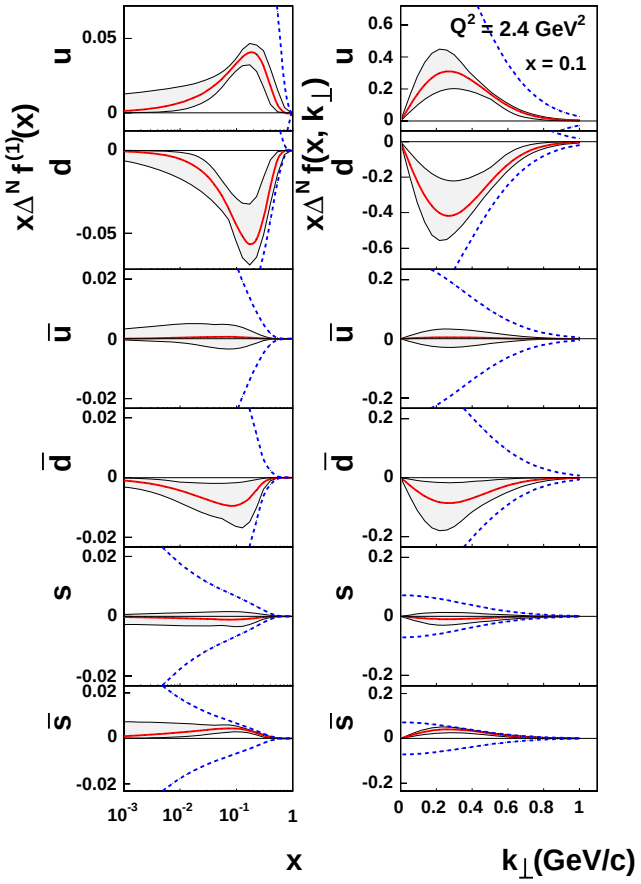

Figure 5. Quark Sivers functions from SIDIS [40].

models, in particular with a bag model and the spectator model with scalar and axial-vector diquarks of Ref. [49]. The results for the pretzelosity distribution and its transverse moments are rather different in different models, and this sensitivity to the adopted model suggests that new data could give useful insights to model the momentum dependence of the nucleon wave function. A preliminary work on the transversity distribution calculated by the Pavia group [53] using the hypercentral wave function [52, 7] shows an interesting and intriguing coincidence with a phenomenological extraction of the transversity distribution.

T-odd functions were calculated in a spectator model with scalar diquarks in [54] and scalar and vector diquarks in [55], in the MIT bag model by Yuan[56] and by Cherednikov, D'Alesio, Kokelev and Murgia [57], in the non relativistic Isgur Karl constituent quark model by the Valencia-Perugia collaboration [58] and in a spectator model for the pion [59].

A calculation of all the TMDs in a spectator model with a scalar diquark can be found in Ref. [60], while in the paper by Bacchetta, Conti and Radici [61] the authors calculate all the TMDs by using also an axial vector diquark. They consider different options for the possible diquark polarization states, as well as for the form factors that parametrize the nucleon quark diquark vertex. Their results for the transversity distributions are given in figures 7 and 8 , that correspond to figures 8 and 9 of Ref. [61]. It is interesting to observe that there is a change

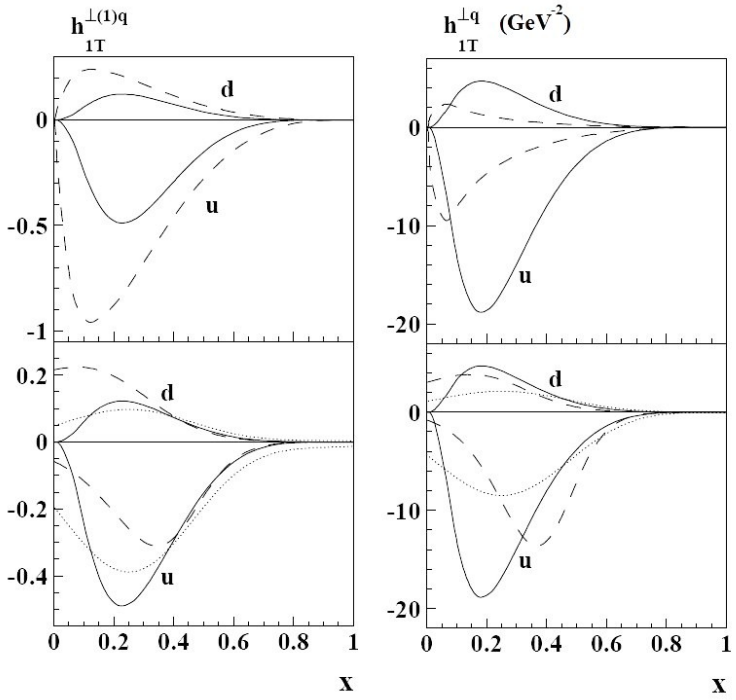

Figure 6. Pretzelosity distribution (left) and the transverse moment of the pretzelosity distribution (right) calculated in different models from Ref. [50] [APS copyright]. Solid curves: light cone calculation with the momentum wave function by Schlumpf [51]. Dashed curves in the upper panels: light cone calculation with the hypercentral model wave function [52, 7]. Dashed curves in the lower panels: results from the spectator model of Ref. [49]. Dotted curves: results from the bag model of Ref. [49].

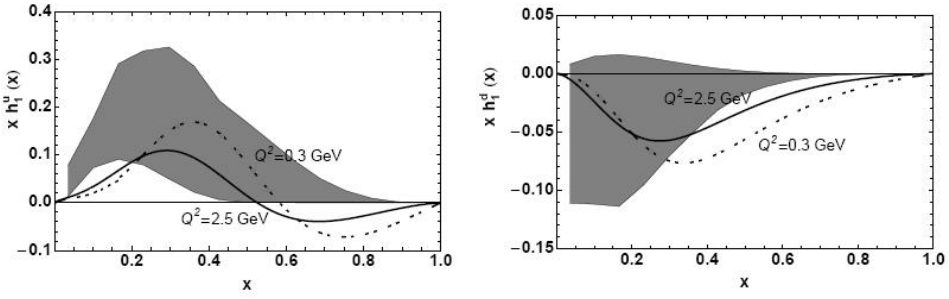

Figure 7. The transversity distribution $xh_1(x)$ for up (left) and down quark (right) from Ref. [61] [APS copyright]. Dashed (Solid) curves for the scalar-vector diquark model before (after) the evolution at LO. Shaded area: uncertainty band in the phenomenological extraction from Ref. [38] .

of sign in the transversity distribution for the up quark, a feature that seems not to be shown by other models. The use of models instead of phenomenological parametrizations, may help to undertand information that are encoded in the TMDs, like their relations with the angular

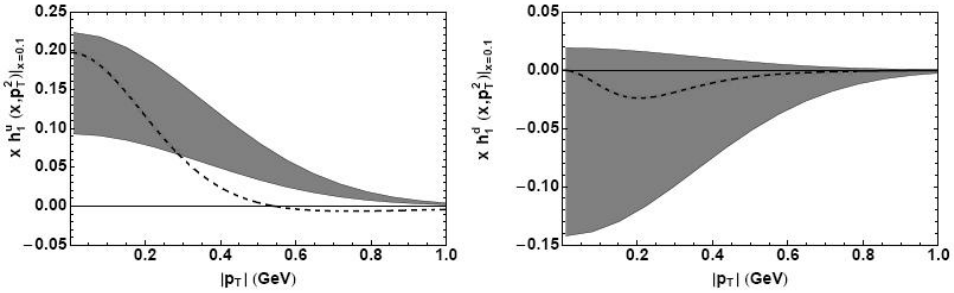

Figure 8. The p_T dependence of the transversity distributions for up (left) and down quark (right) from Ref. [61] [APS copyright]. Dashed curves for the scalar-vector diquark model. Shaded area: uncertainty band in the phenomenological extraction from Ref. [38] .

momenta of the partons and the nucleon deformations. Moreover from an experimental side they could be useful to estimate the size of an observable in different processes and kinematical regimes and to set up Monte Carlo simulations [62].

3.2. Fragmentation functions

A complementary information on the internal structure of hadrons is encoded in the Fragmentation Functions (FFs) involved in the description of semi-inclusive processes with one or more hadrons of the final state detected. In the case of two final hadrons they are called Dihadron Fragmentation Functions (DiFF) and were proposed for the first time in Refs. [63] [64] [65] [66] and then systematically analyzed at leading twist in Ref. [67] and at twist-3 in Ref. [68]. Like the PDFs also the FFs are universal in the sense that they are process independent. They parameterize the process of hadronization, the unknown mechanism by means of which partons (quarks or gluons) turn into confined hadrons in the final state which are observed by the detectors. Clearly they are non perturbative objects, thus they should be modeled or parametrized. Recently a lot of work has been dedicated to DiFF [67][68][69][70][71][72][73]. In principle, although experimentally difficult, the detection of two final state hadrons can give access to information on the spin correlations in the hadronization process in terms of polarized FFs.

As a beautiful example Radici, Jakob and Bianconi have quantitatively demonstrated [70] that in the process $ep \to e'\pi^+\pi^-$ X, with the target proton transversely polarized, it is possible to extract a spin asymmetry that is proportional to the product of the transversity and the DiFF that describes the fragmentation of the polarized parton into two pions. This can be an alternative way to extract the transversity with the advantage in respect to the Collins effect that the process is collinear, the transverse momenta can be integrated out, and the evolution is under control. The first process has been measured at HERMES at $Q^2 = 2.5\ GeV^2$ [75], while the annihilation process will be measured at BELLE at $Q^2 = 100\ GeV^2$. In this context, Bacchetta and Radici have calculated this Dihadron fragmentation function within a diquark spectator model [72], and given prediction for the asymmetry [72] measured at HERMES and finally derived evolution equations for the DiFF in Ref. [73].

In figure 9 (from Ref. [74]), one can compare the predictions by Bacchetta and Radici [72] and the HERMES data [75].

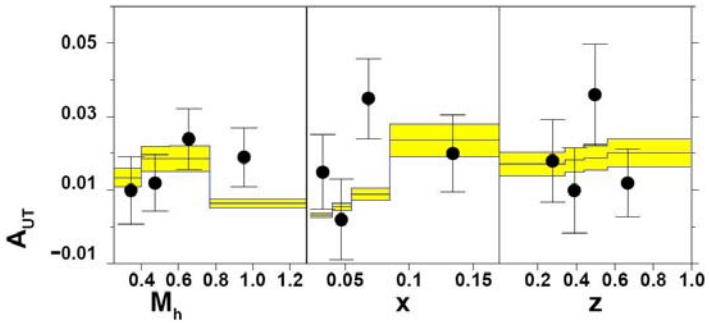

Figure 9. Spin asymmetry for semi-inclusive production of a pion pair in deep-inelastic scattering on a transversely polarized proton as a function of the invariant mass of the pion pair, M_h (GeV), of the light-cone momentum fraction of the initial parton, x, of the energy fraction carried by the pion pair with respect to the fragmenting parton, z, as from Ref. [74] [APS copyright]. Data from Ref.[75]. The uncertainty band is a fit to the data based on the DiFF spectator model of Ref.[72] and on the h_1 parametrization of Ref.[39].

4. Exotic meson states

The exotic meson states are hadrons with zero baryonic number which are not reproducible in the usual quark-antiquark scheme. The exotics which are mainly studied in literature are tetraquarks, hybrids and glueballs.

The tetraquarks are mesons composed of two constituent quarks and two constituent antiquarks. There are three different types of models for tetraquark systems: the uncorrelated, the diquark-antidiquark and the quasi-molecular ones. The group of Genova has developed an algebraic model description for the first two schemes of light tetraquarks for which there are experimental evidences from KLOE, E791 and BES.

The hybrids are mesons with gluonic components. The most commonly studied hybrids are those containing a couple of quark and antiquark and a single (effective, quasi) gluon. There seems to be some evidences of hybrids states in the light quark sector: experiment E852 at BNL have observed $\pi_1(1400)$, $\pi_1(1600)$ and $\pi_1(2000)$ with exotic J^{PC} quantum numbers. The Indiana-Genova collaboration has used the non relativistic reduction of Coulomb gauge QCD to compute the spectrum of the low mass hybrid mesons containing a heavy quark-antiquark pair.The gluon degrees of freedom are treated in the mean field approximation calibrated to the gluelump spectrum. New experiments specifically devoted to the heavy hybrids are to be carried on at Jlab from the Gluex and the Clas collaborations, at PANDA and at BESIII.

The last type of exotic mesons are the glueballs, gluonic colour singlet bound states. There are evidences from the Crystal Barrel collaboration regarding a light scalar glueball $f_0(1500)$ and the PANDA experiment has been designed to discover glueballs up to masses of 4.5 GeV. The group of Trento has studied this resonance in the Interacting Instanton Liquid Model [76].

4.1. Tetraquark states

The quark-antiquark assignment to P-waves [77] has never worked for the lowest lying scalar mesons, $f_0(980)$, $a_0(980)$, $\kappa(800)$ and $f_0(600)$ [78]. Already in the seventies Jaffe [78] suggested the tetraquark structure of the scalar nonet and proposed a four quark bag model. Recently Maiani *et al.* in Ref. [79] have suggested that these mesons could be described as a tetraquark nonet, in particular as a diquark-antidiquark system.

In Ref. [80] a complete classification scheme of the two quark-two antiquark states in terms of $SU(6)_{sf}$ has been published, as well as an evaluation of the tetraquark spectrum for the lowest scalar meson nonet, obtained both in the tetraquark uncorrelated case and in the diquark-antidiquark case using algebraic model tecniques.

In the construction of the classification scheme symmetry principles have been used without introducing any explicit dynamical model. There are two constraints: the tetraquark wave functions should be a colour singlet, as all physical states, and the tetraquarks states must be antisymmetric for the exchange of the two quarks and the two antiquarks.

The allowed $SU(3)_f$ representations for the $qq\bar{q}\bar{q}$ system are $2[1] \oplus 4[8] \oplus [10] \oplus [\overline{10}] \oplus [27]$. The allowed isospin values are $I = 0, \frac{1}{2}, 1, \frac{3}{2}, 2$, while the hypercharge values are $Y = 0, \pm 1, \pm 2$. The values $I = \frac{3}{2}, 2$ and $Y = \pm 2$ are exotic, which means that they are forbidden for the $q\bar{q}$ mesons. The allowed $SU(2)_s$ representations are $2[1] \oplus 3[3] \oplus [5]$. The tetraquarks can have an exotic spin $S = 2$. In Appendices A and B of Ref. [80] all the flavor and spin states in the $qq\bar{q}\bar{q}$ configuration are explicitly written in terms of the single quark and antiquark states. The flavor states are also written in the ideal mixing hypothesys, i.e. as a superposition of the SU(3)-symmetrical states in such a way to have defined strange quark and antiquark numbers.

The spatial, flavor, color and spin parts with given permutational symmetry have been combined together to obtain completely antisymmetric states under the exchange of the two quarks and the two antiquarks. The resulting states are listed in Table III of Ref. [80]. The possible flavor, spin and J^{PC} values can be found in Table V, VI, VII and VIII of Ref. [80] for different orbital angular momenta.

The mass splitting of the candidate tetraquark nonet, i.e. $f_0(980)$, $a_0(980)$, $\kappa(800)$ and $f_0(600)$, see Ref. [80] has been evaluated by means of a mass formula for normal mesons [81] extended to tetraquark systems. The masses of the other mesons belonging to the same tetraquark nonet do not seem in very good agreement with the experimental values, even if, before reaching any conclusion, new experiments, especially on the poorly known $\kappa(800)$ and $f_0(600)$, are mandatory.

The constituent diquark is thought as two correlated constituent quarks with no internal spatial excitations. Thus the tetraquark mesons are described in the diquark-antidiquark limit as composed of a constituent diquark, (qq), and a constituent antidiquark, $(\bar{q}\bar{q})$. The diquark-antidiquark states in this limit are a subset of the tetraquark states previously derived. The spectrum generating algebra is $U(4) \otimes SU(3)_f \otimes SU(2)_s \otimes SU(3)_c$ and the mass formula can be written as:

$$M^2 = (M_{qq} + M_{\bar{q}\bar{q}})^2 + a \cdot n + b \cdot L_{12-34} + c \cdot S_{tot} + d \cdot J, \tag{2}$$

where M_{qq} and $M_{\bar{q}\bar{q}}$ are the diquark and antidiquark masses, n is a vibrational quantum number, L_{12-34} the relative orbital angular momentum, S_{tot} the total spin and J the total angular momentum. The masses for the candidate tetraquark nonet obtained with this model are much closer to the experimental values than the masses obtained in the tetraquark model. However it should be again stressed that, before reaching any conclusion, new experiments are necessary, also to be sure of the existence of all the states of the scalar nonet. If the existence of only some states of the nonet will be confirmed a different kind of clusterization will emerge, and this limit has still to be studied in an algebraic framework.

4.2. The hybrids states

Low energy gluons are responsible for the distinctive features of QCD such as confinement and chiral symmetry breaking. For the purpose of getting insights into the non-perturbative features of QCD, it is possible to design idealized systems that are sensitive to the pure Yang-Mills sector and to bypass many of the complications of the full QCD. A gluelump is an example of such an idealized state. It is a state of the gluon field bound to a static, localized octet source which

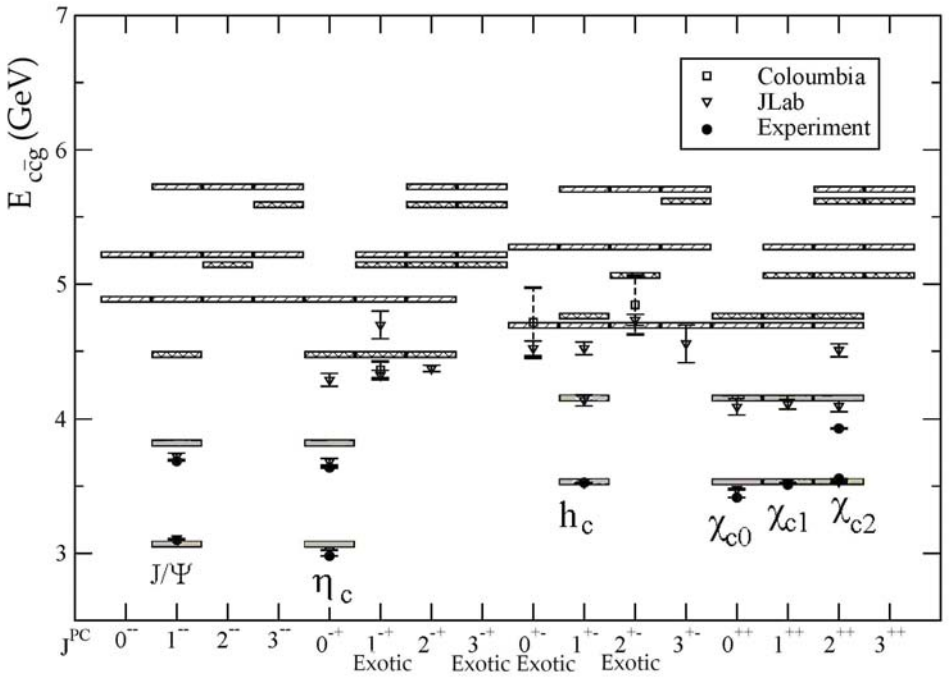

Figure 10. Charmonium (full grey boxes) and charmonium hybrid spectrum (single dashed and double dashed boxes) compared with data (where available) or lattice computations. Single dashed boxes are the $c\bar{c}g$ hybrids dominated by the P-wave quarks, all other have the $Q\bar{Q}$ pair in the relative S-wave orbital. Full grey boxes show results for the spin-averaged masses of ordinary charmonium states. The names of the ordinary charmonium families are also indicated. From Ref. [85][APS copyright].

can be constructed, for example as a quark-antiquark pair placed at an origin. Since the quark and the antiquark are at zero relative separation the system is rotationally symmetric, invariant under parity and charge conjugation. Thus gluelump states can be classified by the same J^{PC} quantum numbers as ordinary mesons.

The gluelump spectrum is studied [82] in the variational approach to Coulomb gauge QCD [83, 84] and massive quasi-gluon excitations are used to construct the Fock space representation. The calculated gluelump spectrum reproduce the spectrum obtained from lattice QCD computations. In particular, the ordering of the levels found in lattice QCD calculations is confirmed and it turns out to be non-trivially related to the non abelian structure of the Coulomb interaction in the Coulomb gauge which leads to three body interaction in the equation for the gluelump energies.

This numerical calculation has been used also to compute the spectrum of low mass hybrid mesons containing a heavy quark-antiquark pair [85], since in this case we can think the states as an external product of the gluelump states and the quark-antiquark states. Using the non relativistic reduction of Coulomb gauge QCD the spectrum of the low mass hybrid mesons containing a heavy quark-antiquark pair is numerically calculated. The gluon degrees of freedom are treated in the mean field approximation calibrated to the gluelump spectrum. Like in the gluelump case the resulting potential from Coulomb gauge QCD has not only a two body interaction, but also a non irreducible three body term linking all three constituents(quasi-particles)– quark, antiquark and gluon. The explicit expression of the two and three body potential can be found in Ref. [85]. It is this three-body interaction, related to the non-Abelian

part of the QCD Coulomb interaction, that is responsible for producing the inverted parity ordering of the charmoniom hybrids spectra, as also seen in LQCD results. The numerical results, for charmonium hybrids, are given in figure 10 and compared with LQCD results.

4.3. Glueballs

The group of Trento has used the Interacting Instanton Liquid Model IILM (for a review on the IILM see Ref. [76]) as a tool to study the role played by the chiral interactions in the lowest-lying vector and axial vector meson resonances, i.e a_1 and ρ [86]. Using the same model, then the group of Trento also analized the properties of the glueballs [87], in particular of the lightest resonance.

Instantons have been long argued to be the dominant fluctuations generating the zero-mode zone of the Dirac operator, hence providing the correlations which break spontaneously chiral symmetry. In the IILM, the QCD path integral over all gluon configurations is replaced by an effective theory in which the gauge fields accounted for are those generated by integrating over the positions, color orientations, and sizes of singular-gauge instantons. The principal flaw of the instanton liquid model is that it does not predict a linearly rising potential between static color sources, at large distances. Thus, although this model describes well the non-perturbative QCD correlations at the chiral symmetry breaking scale $\Lambda_\chi \sim$ 1 GeV, it fails at the confining scale $\sim \Lambda_{QCD} \sim$ 0.2 GeV. Because of the lack of confinement, the IILM can be used as a tool to single-out the contribution of chiral forces in the different hadronic systems by studying where the model works well. In this context, the a_1 and ρ resonances represent good test systems: being in between the pion, strongly related to chiral symmetry breaking, and highly excited states, dominated by color confinement, they are expected to be sensitive to both chiral and confining interactions. In addition the splitting between these two resonance masses can be a measure of the effect of chiral symmetry breaking.

In Ref. [86] momentum projected correlation functions are computed at Euclidean times up to $\sim$ 1.2 fm and the effective mass plot analysis reported. This is done not only for stable states, as in lattice QCD simulations, but also for resonances with a finite width. In the former case the effective mass plot displays a flat plateau in the large Euclidean time limit, while in the latter one displays an approximatively linear and mild fall-off behaviour in the intermediate region. The effective mass plot analysis is applied in particular to determine the mass of the lowest-lying vector and axial-vector mesons, using several values of the quark mass. The results [86] show that the instanton-induced chiral forces are sufficiently strong to generate the ρ and the a_1 mesons even in absence of confinement. On the other hand, the obtained mass values for the vector and axial vector mesons are a 30% greater than the corresponding experimental values,in particular $M_\rho \simeq 1$ GeV and $M_{a_1} \simeq$ 1.7 GeV. Thus the masses of the vector and axial mesons receive significant contributions also from confinement, of the order of 30%. It is important to remind that on the contrary the masses of the lowest states like the pion and the nucleon, as completely dominated by chiral forces, were previously exactly reproduced in this scheme [88].

Lattice studies have found that the lightest glueball should be in the mass range 1.500 − 1.750 GeV and that it should be an unusually compact object,with a size of the order $\sim$ 0.2 fm. Thus, it is reasonable to expect that the dominant forces, responsible for its binding, should act at the chiral symmetry breaking scale, rather than at the confinement scale. In this respect, the IILM should be a suitable tool to study the lightest glueball. Introducing the effective energy $E_{eff}(\tau, \mathbf{p})$ as the logarithmic derivative of the momentum-projected correlation function $G_S(\tau, \mathbf{p})$ [87],

$$E_{eff}(\tau, \mathbf{p}) = -\frac{d}{d\tau} \log G_S(\tau, \mathbf{p}), \tag{3}$$

the spectrum contains a scalar glueball bound-state of mass $M_{0^{++}}$, only if at large Euclidean

times the effective energy $E_{eff}(\tau, \mathbf{p})$ becomes independent on τ and converges to the kinetic energy of such a state, propagating with momentum $\mathbf{p}$:

$$\lim_{\tau\to\infty} E_{eff}(\tau, \mathbf{p}) = \sqrt{\mathbf{p}^2 + M^2_{0^{++}}}. \tag{4}$$

Correlation functions in the IILM can be computed numerically using Monte Carlo methods and the results show (see Ref. [87]) that the momentum projected correlator displays a plateau at large Euclidean times, signature of a bound state existence within this scheme[87]. The masses extracted using different quark masses are in the range $M^{IILM}_{0^{++}} \simeq 1.68 - 1.78$ GeV [87], consistent with the predictions of lattice QCD simulations. A complementary analysis was also carried on in the SIA (Single Instanton Approximation) model. This method offers analytic insight, and is based on the extraction of the mass from effective energy evaluated at finite momentum $\mathbf{p}$. Additional evidence [87] for a bound-state was found with an estimated mass $M^{SIA}_{0^{++}} \simeq 1.29 - 1.42$ GeV, i.e. consistent with the value calculated in lattice gauge theory.

5. Lattice QCD calculations of hadron observables

The European Twisted Mass Collaboration (ETMC) has started a systematic program of calculations of three-point correlation functions using the unquenched gauge configurations produced for different values of the lattice spacing and volumes, adopting the tree-level improved Symanzik gauge action and the twisted mass fermionic action with two dynamical flavors tuned at maximal twist (see Ref. [89]). Their aim is the determination of the electromagnetic and weak form factors of light and heavy-light mesons and baryons. Recently [90] they have calculated the electromagnetic pion form factor for pion masses between 260 MeV and 580 MeV. The lattice spacings are lower than 0.1 fm and the lattice volumes greater than 2 fm^3.

The extrapolation to the physical point is carried out using chiral perturbation theory at NNLO. The pion mass, its decay constant and form factor calculated in the [0.05,0.8]GeV^2 range of Q^2, are all simultaneously fitted. The low-energy constants extracted from the chiral fit are in agreement with those obtained in a chiral analysis of pion-pion scattering data [91]. The comparison between the chiral extrapolation of the ETMC results (full dots) and the experimental data (open markers) is shown in figure 11, where the dashed lines correspond to the chiral fit uncertainty (statistical plus systematic). As one can check, there is a very good agreement between the chiral extrapolation of the ETMC lattice results [90] and the experimental data [59]. The use of all-to-all quark propagators computed with a stochastic method, as well as of twisted boundary conditions on the valence quark fields, has allowed to achieve a remarkable statistical precision and very low values of the four momentum transfer, giving the possibility of an accurate chiral extrapolation of the calculated form factor to the physical point.

6. Quark-antiquark and/or meson cloud effects

We have already discussed the open problem of the missing strength in the theoretical prediction for the electromagnetic excitation of the baryon resonances with constituent quark models, that indicates that some fundamental mechanism is lacking in the dynamical description of the nucleon structure. This mechanism can be identified with the production of a quark-antiquark pair [18, 20]. A strong interest on the possible influence of such quark-antiquark and/or meson cloud effects is emerging in the literature. The problem is how to include this feature into the description of hadrons. A possibility is to introduce higher Fock components in the hadron wave function. This means that, at the hadron scale, the baryon acquires a $4q\bar{q}$ configuration

$$\mid \Psi\rangle = \Psi_{qqq} \mid qqq\rangle + \Psi_{4q\bar{q}} \mid qqq\bar{q}q\rangle \tag{5}$$

The consistent inclusion of higher Fock components in CQMs is a hard task, but, as a preliminary approach one can introduce models in which the physical nucleon N is considered

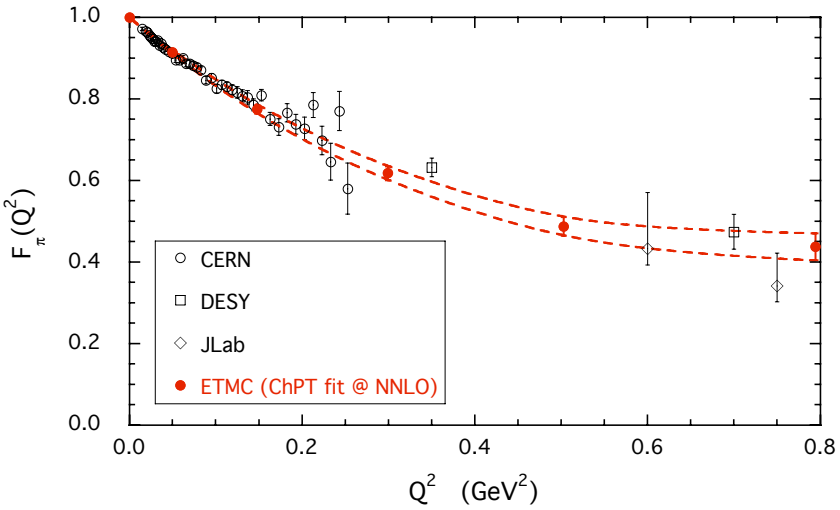

Figure 11. Charge form factor of the pion versus Q^2. The chiral extrapolation of the ETMC lattice results (full dots) Ref. [90] is compared with the experimental data (open markers) Ref. [92]. The dashed lines correspond to the region selected at 1σ level by the NNLO chiral analysis.

to be made of a bare nucleon dressed by a surrounding meson cloud

$$\mid N\rangle = \Psi_{3q} \mid N(qqq)\rangle + \sum\nolimits_{B,M} \Psi_{(3q)(q\bar{q})} \mid B(qqq)M(q\bar{q})\rangle + ... \tag{6}$$

An approach of this type has been used by the Pavia group to calculate GPDs[93]. The virtual photon can scatter either on a valence quark of the bare nucleon, or on one of the quarks in the baryon-, B, or meson-, M, clusters that form the higher Fock state (BM). The calculations are done considering the possibility of two higher Fock states, pion-nucleon and Delta-nucleon, using a light cone hamiltonian with hypercentral interaction [52, 7] and a direct pion-nucleon(Delta) coupling. The GPDs are calculated by means of the convolution formalism. The results for the isoscalar and isovector unpolarized and helicity GPDs are shown in figure 12 using light cone wave functions from the hypercentral model for the nucleon [52, 7] and a gaussian for the pion.

In another similar approach in a Beijin-Genoa collaboration, using the hCQM [94] wave functions, the pion cloud has been added by means of the pion-nucleon coupling taken from [95]. The preliminary results show that the higher Fock components give relevant contributions both to the elastic form factors of the nucleon and to helicity amplitudes [94].

The contributions of the higher Fock components to the pion form factor have been calculated by the Rome group [96]. The photon vertex is dressed by means of a covariant vector meson dominance and a direct pion absorption by quarks is considered. Among the various terms contributing to the electromagnetic amplitude, the so called instantaneous terms seem to be of relevant importance. An important aspect of the approach is that a unified description of both time- and space-like form factors can be obtained. The theoretical results [96], in comparison to the experimental data, are shown on figure 13. The agreement is impressive. A similar calculation has been done also for the nucleon form factors [97].

All these approaches describe the pairs as mesons that couples to the hadrons. A sistematic inclusion of a quark antiquark pair-creation mechanism at the quark level is not yet available. A possibility is given by a recent work aiming at unquenching the quark model [98]. The $q\bar{q}$ creation mechanism is introduced at the quark level by means of a QCD inspired $3P0$ mechanism. The construction of the formalism and the difficult linked problems have been solved by means of

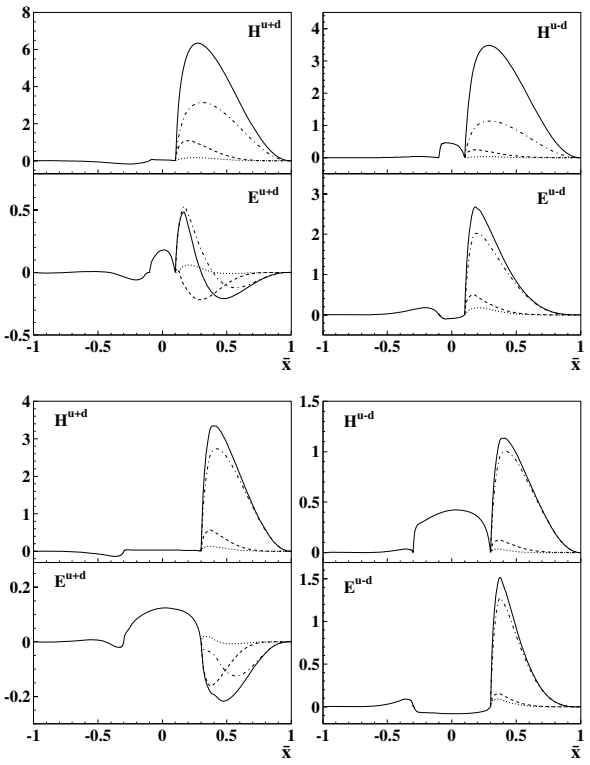

Figure 12. Isoscalar $(u+d)$ and isovector $(u-d)$ of the averaged $H-$ and $E-$ type GPDs calculated in a meson-cloud convolution for $t=-0.5\ GeV^2$ and $\xi=0.1$ (upper part) or $\xi=0.3$ (lower part) from Ref. [93] [APS copyright].

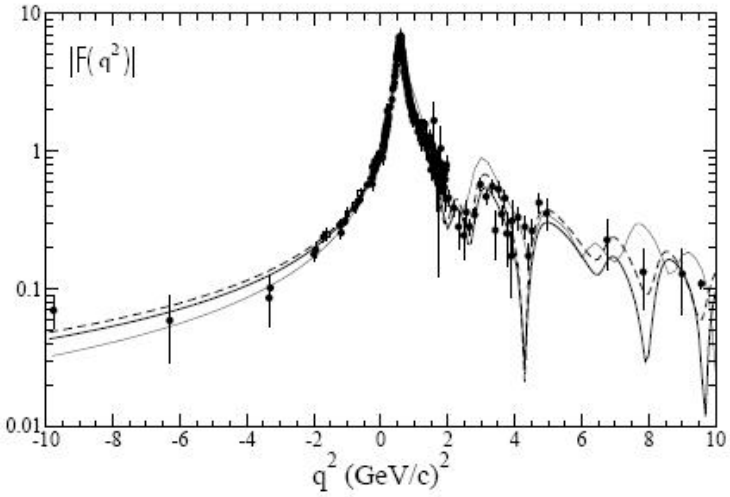

Figure 13. The pion form factor in the time- and space-like regions as from Ref. [96] [APS copyright] compared with data (details and data in the article).

group theory. In fact the sum over all big towers of intermediate states has been performed thanks to group theoretical methods and the permutational symmetry for all identical quarks has been taken into account. All the possible intermediate states are considered, since as Isgur has shown some years ago, no truncated Fock space can preserve the good CQM results for meson spectroscopy and the OZI hierarchy. Preliminary results for the proton spin show that one half is carried by valence quarks and the other one half is due to the orbital angular momenta of the quark-antiquark pairs [98].

Acknowledgements
The author is indebted with the colleagues working in the Universities and/or INFN Sections of Genova, Roma1-2-3, Pavia, Perugia, Trento for supplying their results and sending materials useful for the preparation of her talk and this contribution.

References

[1] 2004 *Hadronic Physics from Lattice QCD*, ed A M Green (Singapore:Word Scientific)
[2] Bijnens J 2007 *Prog. Part. Nucl. Phys.* **58** 521
[3] Morpurgo G 1965 *Physics* **2** 95
[4] Isgur N and Karl G 1979 *Phys. Rev.* D **18** 4187; *Phys. Rev.* D **19** 2653
[5] Capstick S and Isgur N 1986 *Phys. Rev.* D **34** 2809
[6] Bijker R, Iachello F and Leviatan A 1994 *Ann. Phys. (N.Y.)* **236** 69
[7] Ferraris M, Giannini M M, Pizzo M, Santopinto E and Tiator L 1995 *Phys. Lett.* B **364** 231
[8] Glozman L Ya and Riska D O 1996 *Phys. Rep.* C **268** 263; Glozman L Ya, Plessas W, Varga K and Wagenbrunn R F 1998 *Phys. Rev.* D **58** 094030.
[9] Löring U, Kretzschmar K, Metsch B Ch and Petry H R 2001 *Eur. Phys. J.* A **10** 309; Löring U, Metsch B Ch and Petry H R 2001 *Eur. Phys. J.* A **10** 395; 447
[10] Thomas A W and Weise W 2001 *The structure of the nucleon* (Berlin:Wiley-VCH)
[11] Schaefer T and Shuryak E 1996 *Phys. Rev.* D **53** 6522; 1998 *Rev. Mod. Phys.* **70** 323; Diakonov D 2003 *Prog. Part. Nucl. Phys.* **51** 173
[12] Cardarelli F, Pace E, Salmé G and Simula S 1995 *Phys. Lett.* B **357** 267.
[13] De Sanctis M, Santopinto E and Giannini MM 1998 *Eur. Phys. J.* A **1** 187.
[14] Pace E, Salmé G, Cardarelli F and Simula S 2000 *Nucl. Phys.* A **666** 33.
[15] De Sanctis M, Giannini M M , Repetto L and Santopinto E 2000 *Phys. Rev.* C **62** 025208.
[16] Boffi S, Glozman L Y, Klink W, Plessas W, Radici M and Wagenbrunn R F 2002 *Eur. Phys. J.* A **14** 17
[17] De Sanctis, Giannini M M, Santopinto E and Vassallo A 2007 *Phys. Rev.* C **76** 062201(R)
[18] Aiello M, Ferraris M, Giannini M M, Pizzo M and Santopinto E 1996 *Phys. Lett.* B **387** 215
[19] De Sanctis M, Santopinto E and Giannini MM 1998 *Eur. Phys. J.* A **2** 403
[20] Aiello M, Giannini M M and Santopinto E 1998 *J. Phys. G: Nucl. Part. Phys.* **24** 753
[21] Koniuk R and Isgur N 1980 *Phys. Rev.* D **21** 1868
[22] Copley L A, Karl G and Obryk E 1969 *Phys. Lett.* **29** 117
[23] Giannini M M and Santopinto E to be published
[24] Burkert V 2003 *Baryons 2002* (Singapore: World Scientific) 29
[25] Tiator L, Drechsel D, Kamalov S, Giannini M M, Santopinto E and Vassallo A 2004 *Eur. Phys. J.* A **19** 55
[26] Drechsel D, Hanstein O, Kamalov S and Tiator L 1999 *Nucl. Phys.* A **645** 145
[27] Kamalov S, Yang SN, Drechsel D, Hanstein O and Tiator L 2001 *Phys. Rev.* C **64** 032201
[28] Yao W -M *et al* 2006 *Particle Data Group J. Phys.* G **33** 1
[29] Sivers D W 1990 *Phys. Rev.* D **41** 83; 1991 *Phys. Rev.* D **43** 261
[30] Anselmino M, Boglione M and Murgia F 1995 *Phys. Lett.* B **362** 164
[31] Anselmino M and Murgia F 1998 *Phys. Lett.* B **442** 470
[32] Mulders P J and Tangerman R D, 1996 *Nucl. Phys.* B **461** 197; Boer D and Mulders P J 1998 *Phys Rev.* D **57** 5780
[33] Brodsky S J, Hwang D S and Schmidt I 2002 *Phys. Lett.* B **530** 99
[34] Brodsky S J, Hwang D S and Schmidt I 2002 *Nucl. Phys.* B **642** 344
[35] Collins J C 2002 *Phys. Lett.* B **536** 43
[36] Anselmino M, Boglione M, D'Alesio U, Leader E, Melis S and Murgia F 2006 *Phys. Rev.* D **73** 014020
[37] D'Alesio U and Murgia F 2004 *Phys. Rev.* D **70** 074009

[38] Anselmino M, Boglione M, D'Alesio U, Kotzinian A, Murgia F, Prokudin A and Turk C 2007 *Phys. Rev.* D **75** 054032
[39] Anselmino M, Boglione M, D'Alesio U, Kotzinian A, Melis S, Murgia F, Prokudin A and Turk C 2008 *16th International Workshop on Deep Inelastic Scattering (DIS 2008)* (*Preprint* hep-ph/08070173)
[40] Anselmino M *et al* 2009 *Eur. Phys. J.* A **39** 89
[41] Anselmino M *et al* 2005 *Phys. Rev.* D **72** 094007
[42] Boglione M, D'Alesio U, Murgia F 2008 *Phys. Rev.* D **77** 051502
[43] Adam D L *et al* (E704 Collaboration) 1991 *Phys. Lett.* B **264** 462, Adams J *et al* (STAR Collaboration) 2004 *Phys. Rev. Lett.* **92** 171801; Adler SS *et al*(PHENIX Collaboration) 2005 *Phys. Rev. Lett.* **95** 202001
[44] Arapetian A *et al* (HERMES Collaboration) 2004 *Phys. Rev. Lett.* **94** 012002; Alexahakhin V Y *et al* (COMPASS Collaboration) 2005 *Phys. Rev. Lett.* **94** 202002; Ageev E S*et al* (COMPASS Collaboration) 2007 *Nucl. Phys.* B **765** 31
[45] Qiu J-W and Sterman G 1998 *Phys. Rev.* D **59** 014020; Kouvaris C, Qiu J-W, Vogelsang W and Yuan F 2006 *Phys. Rev.* D **74** 114013
[46] Bacchetta A, Bomhof C, D'Alesio U, Mulders P J and Murgia F 2007 *Phys. Rev. Lett.* **99** 212002
[47] Bacchetta A, Bomhof C J, Mulders P J and Pijlman F 2005 *Phys. Rev.* D **72** 034030
[48] Mulders PJ and Tangerman RD 1996 *Nucl. Phys.* B **461** 197; Erratum 1997 *Nucl. Phys.* B **484** 538; Boers D Mulders PJ 1998 *Phys. Rev.* D **57** 5780; Goeke K, Metz A and Schlegel 2005 *Phys. Lett.* B **618** 90; Bacchetta A, Diehel M, Goeke K, Metz A, Mulders P J and M Schlegel 2007 *J. High Energy Phys.* JHEP02(2007)093
[49] Jacob R, Mulders PJ and Rodrigues J 1997 *Nucl. Phys.* A **626** 937
[50] Pasquini B, Cazzaniga S and Boffi S 2008 *Phys. Rev.* D **78** 034025
[51] Schlumpf F 1992 doctoral thesis, University of Zurigo, *Preprint* hep-ph/9211255
[52] Faccioli P, Traini M and Vento V 1999 *Nucl. Phys.* A **656** 400
[53] Pasquini B, Pincetti M and Boffi S 2005 *Phys.Rev.* D **72** 094029; 2007 *Phys. Rev.* D **76** 034020
[54] Brodsky S J, Hwang D S and Schmidt I 2002 *Phys. Lett.* B **530**99
[55] Gamber L P, Godstein G R and Schlegel M 2008 *Phys. Rev.* D **77** 094016
[56] Yuan F 2003 *Phys. Lett.* B **575** 45
[57] Cherednikov O I, D'Alesio U, Kochelev N I and Murgia F 2006 *Phys. Lett.* B **642** 39
[58] Courtoy A, Fratini F, Scopetta S and Vento V 2008 *Phys. Rev.* D **78** 034002
[59] Lu Z and Ma B -Q 2004 *Phys. Rev.* D **70** 094044
[60] Meissner S, Metz A and Goeke K 2007 *Phys. Rev.* D **76** 034002
[61] Bacchetta A, Conti F and Radici M 2008 *Phys. Rev.* D **78** 074010
[62] Bianconi A and Radici M 2005 *Phys. Rev.* D **71** 074014; 2005 *Phys. Rev.* D **72** 074013; 2006 *Phys. Rev.* D **73** 034018
[63] Konishi K Ukawa A and Veneziano G 1978 *Phys. Lett.* B **78** 243
[64] Collins J C and Ladinsky G A 1994 *Preprint* hep-ph/9411444; Collins J C Heppelmann S F and Ladinsky G A 1994 *Nucl. Phys.* B **420** 565
[65] Artru X and Collins J C 1996 *Z. Phys.* C **69** 277
[66] Jaffe R L Jin X and Tang J 1998 *Phys. Rev. Lett.* **80** 1166
[67] Bianconi A, Boffi S, Jakob R and Radici M 2000 *Phys. Rev.* D **62** 034008
[68] Bacchetta A and Radici M 2004 *Phys. Rev.* D **69** 074026
[69] Bianconi A, Boffi S, Jakob R and Radici M 2000 *Phys. Rev.* D **62** 034009
[70] Radici M, Jakob R and Bianconi A 2002 *Phys. Rev.* D **65** 074031
[71] Bacchetta A and Radici M 2003 *Phys. Rev.* D **67** 094002
[72] Bacchetta A and Radici M 2006 *Phys. Rev.* D **74** 114007
[73] Ceccopieri F A, Radici M and Bacchetta A 2007 *Phys. Lett.* B **650** 81
[74] Bacchetta A, Ceccopieri F A, Mukherjee A and Radici M 2009 *Phys. Rev.* D **79** 034029
[75] Airapetian A*et al* (*HERMES Collaboration*) 2008 *J. High Energy Phys.* JHEP06(2008)017
[76] Schaefer T and Shuryak E V 1998 *Rev. Mod. Phys.* **70** 323
[77] Tornqvist N A 1995 *Z. Phys.* C **68** 647
[78] Jaffe R L 1977 *Phys. Rev.* D **15** 267
[79] Maiani L, Piccinini F, Polosa A D and Riquer V 2004 *Phys. Rev. Lett.* **93** 212002
[80] Santopinto E and Galatà G 2007 *Phys. Rev.* C **75** 045206
[81] Iachello F and Mukhopadhyay N C and Zhang L 1991 *Phys. Lett.* B **256** 295
[82] Guo P, Szczepaniak A P, Galata G, Vassallo A and Santopinto E 2008 *Phys. Rev.* D **77** 056005
[83] Szczepaniak A P and Swanson E S 2002 Phys. Rev. D **65** 025012
[84] Feuchter C and Reinhardt H 2004 Phys. Rev. D **70** 105021; Reinhardt H and Feuchter C 2005 Phys. Rev. D **71** 105002

[85] Guo P, Szczepaniak A P, Galata G, Vassallo A and Santopinto E 2008 *Phys. Rev.* D **78** 056003
[86] Cristoforetti M, Faccioli P and Traini M 2007 *Phys. Rev.* D **75** 054024
[87] Tichy M C and Faccioli P 2007 *Preprint* hep-ph/0711.3829
[88] Cristoforetti M, Faccioli P, Negele J and Traini M 2007 *Phys. Rev.* D **75** 034008
[89] Boucaud Ph *et al* (*ETM Coll.*) 2007 *Phys. Lett.* B **650** 304; 2008 *Comput. Phys. Commun.* **179** 695
[90] Frezzotti R, Lubicz V and Simula S 2008 (*ETMC Coll.*) (*Preprint* hep-lat/08124042) ; Simula S (*ETMC Coll.*) 2007 *PoS LATT2007* 371 (*Preprint* hep-lat/07100097)
[91] Colangelo G, Gasser J and Leutwyler H 2001 *Nucl. Phys.* B **603** 125
[92] Amendolia S R *et al* 1986 *Nucl. Phys.* B **277** 168; Ackermann H *et al* 1978 *Nucl. Phys.* B **137** 294; Brauel P *et al* 1979 *Z. Phys.* C **3** 101; Volmer J *et al* (*JLab F(pi) Coll.*) 2001 *Phys. Rev. Lett.* **86** 1713; Tadevosyan V *et al* (*JLab F(pi) Coll.*) 2007 *Phys. Rev.* C **75** 055205; Horn T *et al* (JLab F(pi)-2 Coll.) 2006 *Phys. Rev. Lett.* **97** 192001; Horn T *et al* 2008 *Phys. Rev.* C **78** 058201 ; Huber G M *et al* 2008 *Phys. Rev.* C **78** 045203
[93] Pasquini B and Boffi S 2006 *Phys. Rev.* D **73** 094029
[94] Chen D Y, Dong Y B, Giannini M M and Santopinto E 2007 *Nucl. Phys.* A **782** 62
[95] Theberge S and Thomas A W 1983 *Nucl. Phys.* A **393** 252
[96] De Melo J P B C, Frederico T, Pace E and Salmé G 2006 *Phys. Rev.* D **73** 074013
[97] De Melo J P BC, Frederico T , Pace E, Pisano S and Salmé G 2009 *Phys. Lett.* B **671** 153; 2007 *Nucl. Phys.* A **782** 69
[98] Santopinto E and Bijker R 2008 *Proc. 6th Int. Conf. on Perspective in Hadronic Physics*, ed S Boffi *et al* (Trieste) *AIP Conf. Proc.* vol 1056 (Melville: American Inst. of Phys.) pp 95-97 ; 2008 *Few-Body Syst.* **44** 95